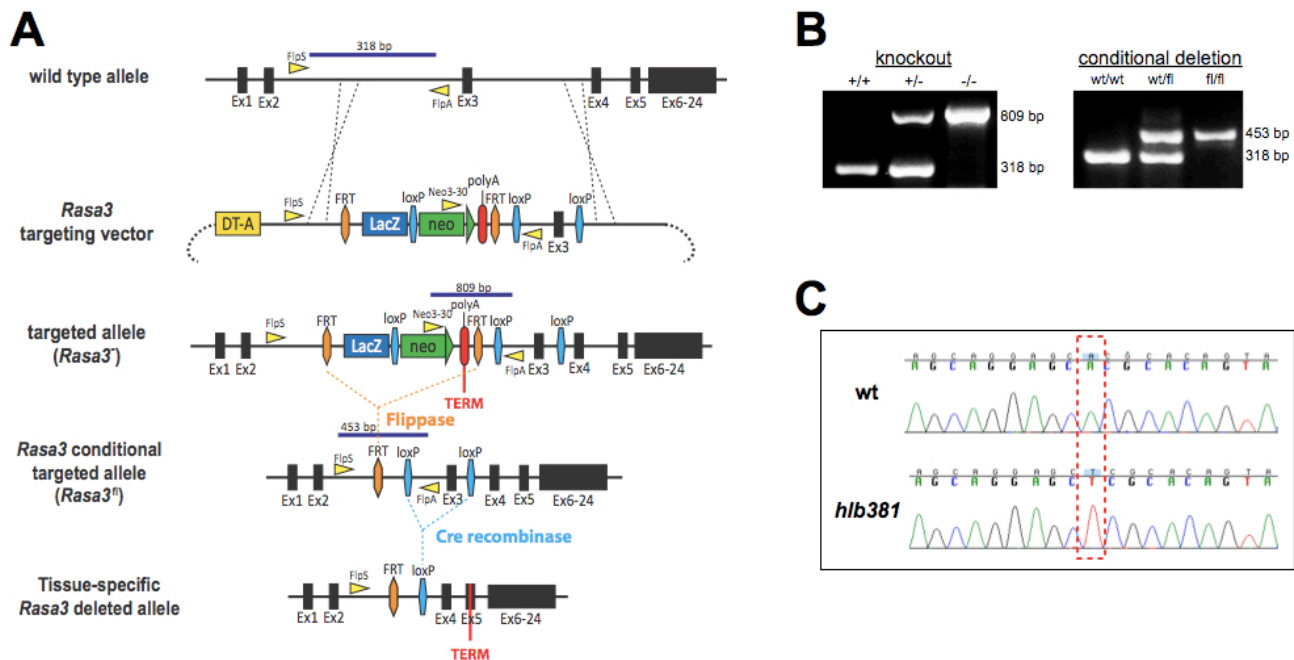
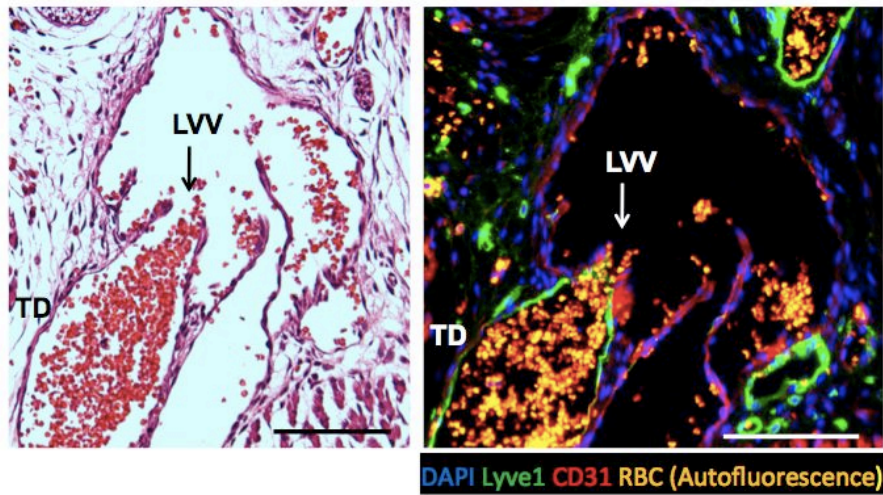


## Supplementary Figure 1



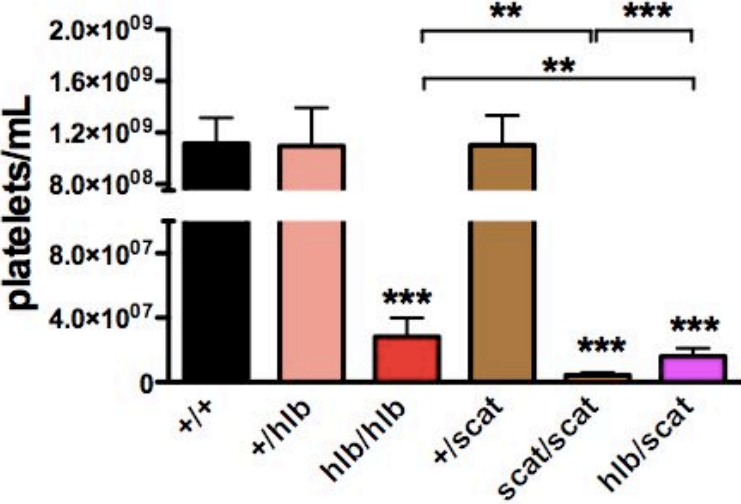
**Generation of *Rasa3* knockout mice. (A)** Scheme of the targeting strategy. The *Rasa3* targeting vector consists of an IRES/LacZ reporter and a promoter-driven neomycin selection marker (Neo) flanked by FRT sites, inserted upstream of a loxP-flanked exon 3 ([http://www.mousephenotype.org/martsearch\\_ikmc\\_project/martsearch/ikmc\\_project/48704](http://www.mousephenotype.org/martsearch_ikmc_project/martsearch/ikmc_project/48704)). The first allele to be generated was a non-expressive form (*Rasa3<sup>fl</sup>*) since the LacZ/Neo cassette has a strong polyadenylation signal that truncates the *Rasa3* mRNA upstream of exon 3 (TERM). Chimeric mice bearing the *Rasa3<sup>fl</sup>* allele were crossed with germline deleter Flp mice to remove the LacZ/Neo cassette and create the conditional *Rasa3* allele (*Rasa3<sup>fl/fl</sup>*) that restores wild type RASA3 expression. Subsequently conditional *Rasa3<sup>fl/fl</sup>* mice were crossed with mice expressing the Cre recombinase under the megakaryocyte-specific Pf4 promoter. Cre-mediated recombination results in excision of exon 3, a frameshift throughout exon 4, and the generation of a premature stop codon in exon 5 that leads to nonsense-mediated mRNA decay. **(B)** Genotyping of *Rasa3* knockout mice. Genomic DNA isolated from tail snips of the indicated mice was analyzed by PCR using the primer pairs shown in (A). **(C)** Identification of the *h1b381* mutation. The mutation in *h1b381* was fine-mapped in an F2 intercross to an interval on mouse chromosome 8 that overlapped the *scat* critical interval. Following positive allele testing with *scat*, we sequenced *Rasa3* in *h1b381* homozygotes to identify the mutation. For sequencing, oligonucleotides were designed using public sequence data (Ensembl, <http://www.ensembl.org>; NCBI, <http://www.ncbi.nlm.nih.gov>). PCR amplification products were purified (AMPure; Agencourt Biosciences) and sequenced using the automated dye termination technique (ABI Prism Model 3700 genetic analyzer; Applied Biosystems). Sequences were analyzed with Sequencher 4.1 licensed software.

## Supplementary Figure 2



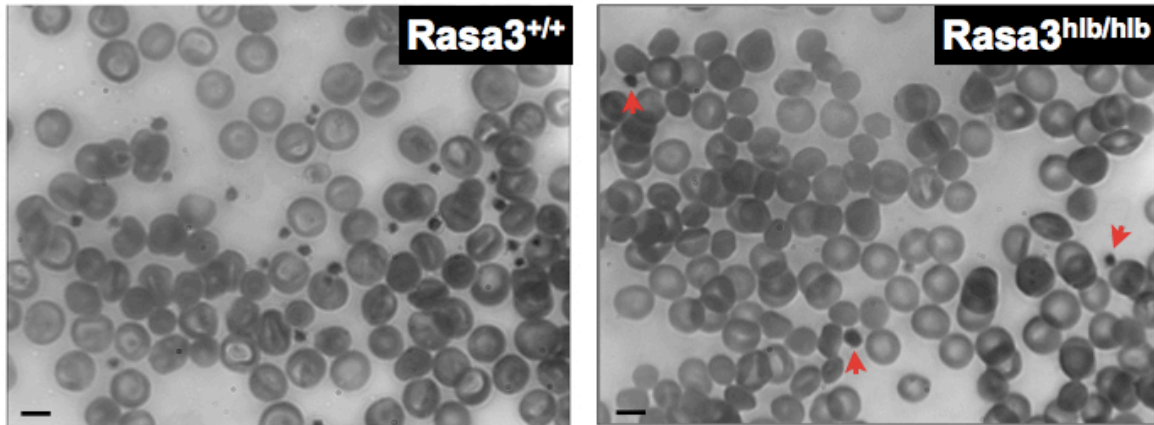
**Lympho-venous junction of a *Rasa3<sup>fl/fl</sup>PF4-Cre<sup>+</sup>* embryo in the transverse plane.** Left: H&E stained section. Right: Sample stained for LYVE-1 (green) to label lymphatic vessels, and CD31 (red) to label blood vessels, along with DAPI staining (blue) and autofluorescent RBCs (yellow) reveals a physical connection between blood and lymphatic vessels allowing blood backflow into the thoracic duct. LVV, lympho-venous valve; TD, thoracic duct. Scale bars represent 100  $\mu\text{m}$ .

Supplementary Figure 3



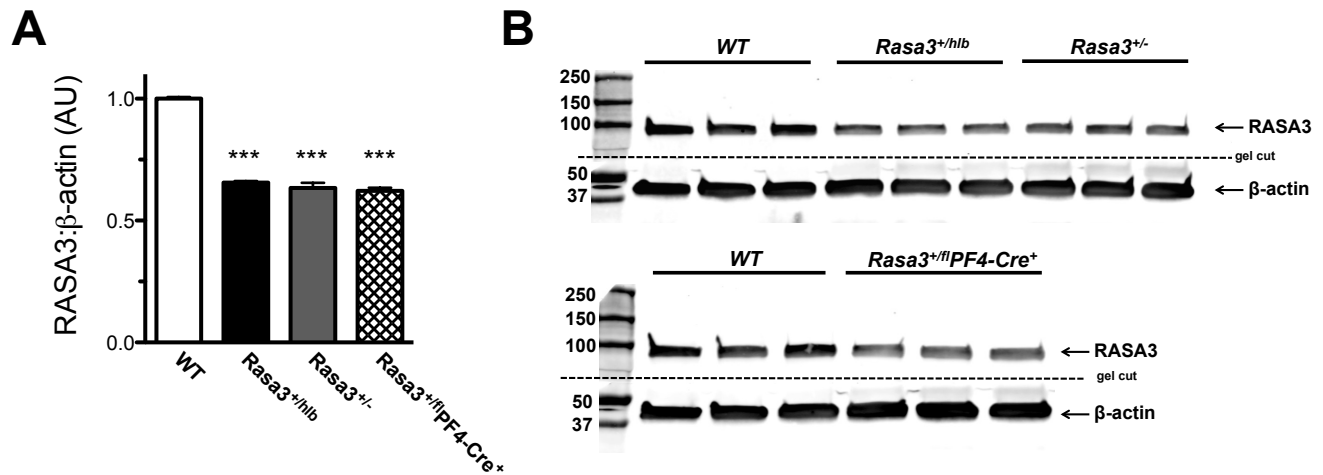
**Peripheral platelet counts in mice of the indicated genotypes.** Note the severe thrombocytopenia in compound heterozygous *Rasa3<sup>hlb/scat</sup>* mice. Statistical significance was determined by 2-way ANOVA with Bonferroni posttest. (n=10 – 23).

## Supplementary Figure 4



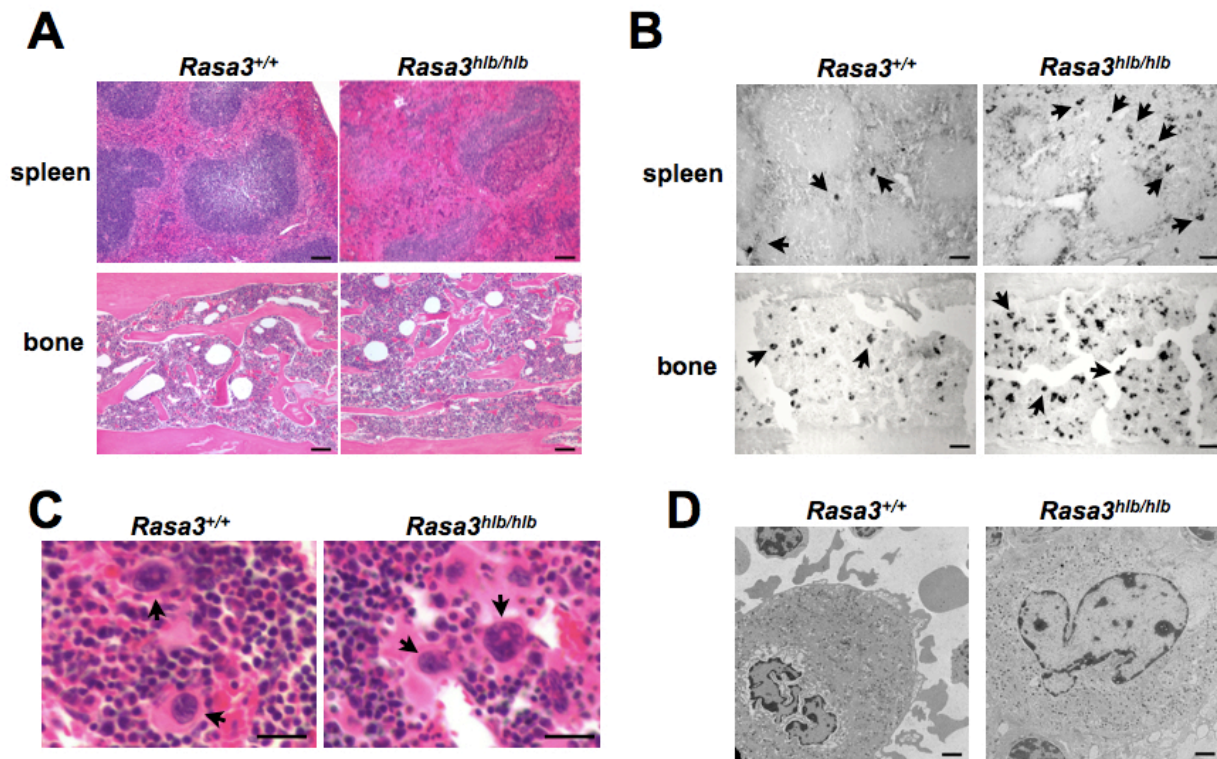
**Blood smears from *Rasa3*<sup>+/+</sup> and *Rasa3*<sup>hlb/hlb</sup> mice.** The red arrows point to the few platelets observed in blood from *Rasa3*<sup>hlb/hlb</sup> mice. Scale bar = 5  $\mu$ m. Results are representative of 3 independent experiments.

## Supplementary Figure 5



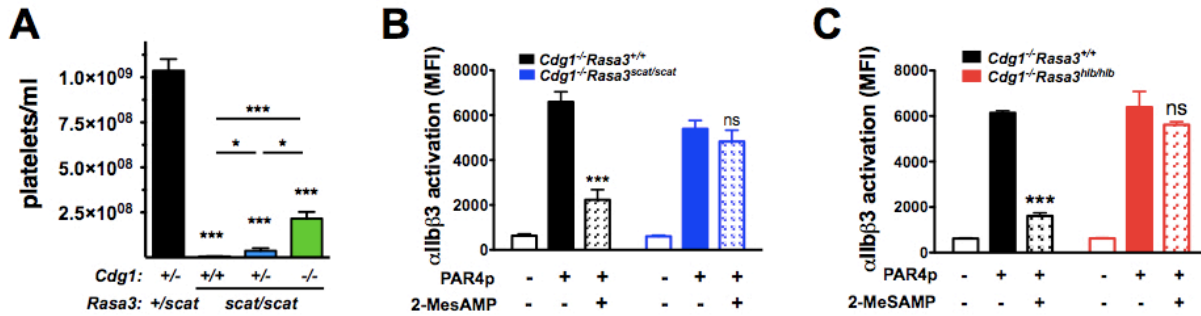
**Reduced RASA3 expression in platelets from *Rasa3*<sup>+/*hib*</sup> mice.** (A) Quantification of RASA3 protein expression relative to β-actin levels in platelets from the indicated genotypes. Note the marked reduction in the RASA3 level of platelets from *Rasa3*<sup>+/*hib*</sup> mice, comparable to that observed in *Rasa3*<sup>+/-</sup> or *Rasa3*<sup>+/*fl*</sup>PF4-Cre<sup>+</sup> platelets. RASA3 expression in *Rasa3*<sup>+/*fl*</sup>PF4-Cre<sup>+</sup> platelets was comparable to that in WT control platelets (not shown). Statistical significance was determined by 2-way ANOVA with Bonferroni posttest. (n = 5). (B) Representative Western blot for RASA3 and β-actin in platelet lysates from three WT, *Rasa3*<sup>+/*hib*</sup>, *Rasa3*<sup>+/-</sup>, and *Rasa3*<sup>+/*fl*</sup>PF4-Cre<sup>+</sup> mice.

## Supplementary Figure 6



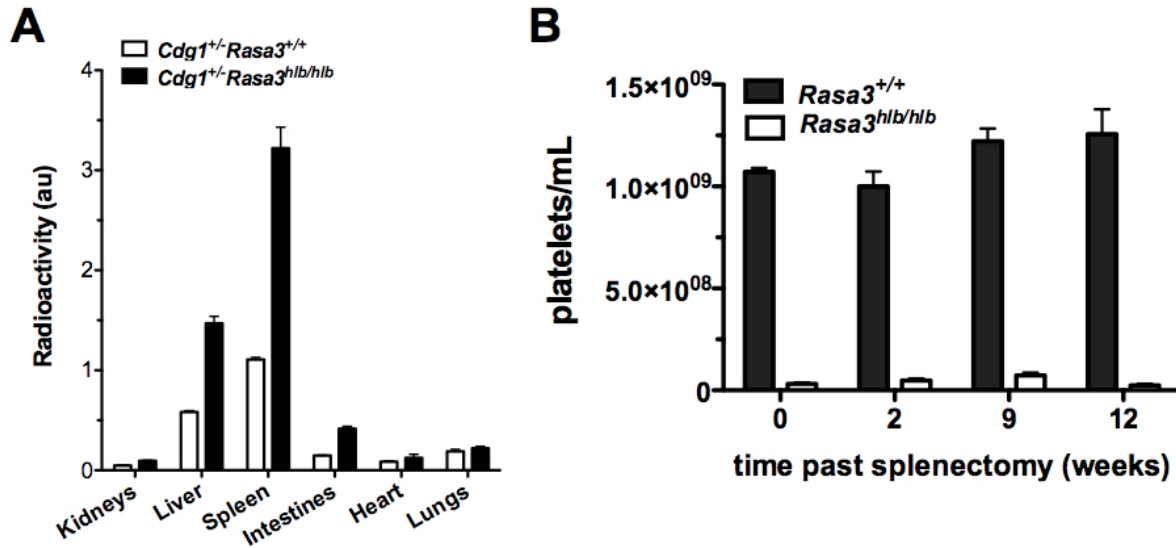
**Expansion of mature megakaryocytes in spleen and bone of *Rasa3*<sup>hlb/hlb</sup> mice. (A)** H&E (Hematoxylin and Eosin) stained sections of spleens (upper panels) and femurs (lower panels) isolated from 3 month-old *Rasa3*<sup>+/+</sup> or *Rasa3*<sup>hlb/hlb</sup> mice; scale bar = 100  $\mu$ m. **(B)** Cryosections of spleens (upper panels) and bones (lower panels) stained for acetylcholinesterase. Arrows point to megakaryocytes; scale bar = 100  $\mu$ m. **(C,D)** No systematic differences in spleen megakaryocyte morphology (C; arrows point to megakaryocytes; scale bar = 50  $\mu$ m) and bone megakaryocyte ultrastructure (D; scale bar = 2  $\mu$ m) were observed. Images are representative for three independent experiments.

## Supplementary Figure 7



**Platelet count and integrin activation response in *Rasa3*<sup>scat</sup> and *Rasa3*<sup>hib</sup> mice. (A)** Peripheral platelet count in *Rasa3*<sup>scat/scat</sup> mice is partially restored by reducing CalDAG-GEFI expression. *Rasa3*<sup>scat/scat</sup> mice were crossed with *Caldaggef1*<sup>-/-</sup> mice and the platelet count was determined by flow cytometry in whole blood isolated from the indicated genotypes. Statistical significance was determined by 2-way ANOVA with Bonferroni posttest. \*p<0.05, \*\*\*p<0.0001. (n = 6). **(B,C)** Agonist-induced αIIbβ3 activation in RASA3 mutant platelets is insensitive to P2Y12 inhibition. Flow cytometry analysis of αIIbβ3 activation (JON/A-PE binding) in *Caldaggef1*<sup>-/-</sup> (*Cdg1*<sup>-/-</sup>, black bars), *Caldaggef1*<sup>-/-</sup> *Rasa3*<sup>scat/scat</sup> (blue bars) or *Caldaggef1*<sup>-/-</sup> *Rasa3*<sup>hib/hib</sup> (red bars) platelets stimulated with 250 μM PAR4p in the presence (checkered bar) or absence (solid bar) of 2-MeSAMP (100 μM). Statistical significance between platelets activated in the presence or absence of 2-MeSAMP was determined by student t-test. \*\*\*p<0.0001; ns: p>0.05. (n = 6).

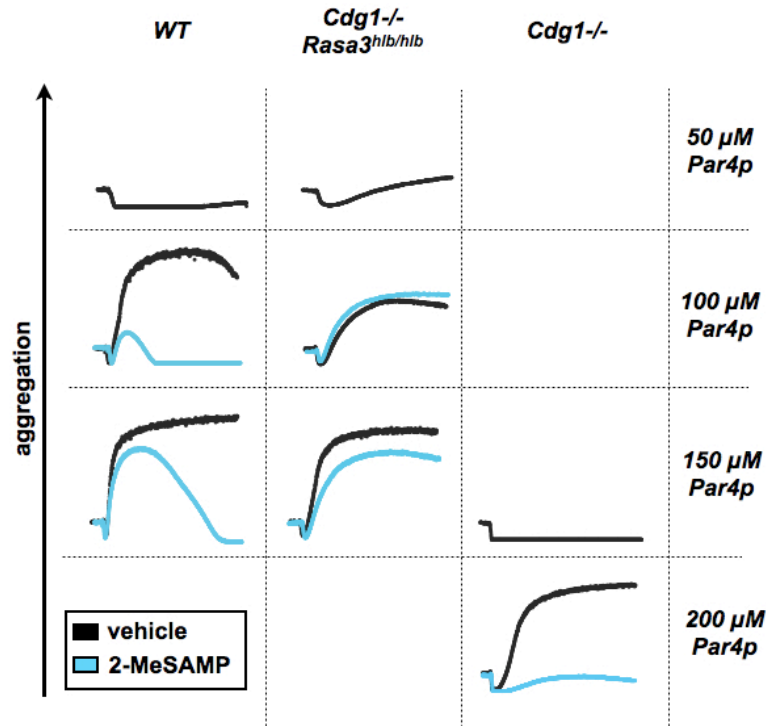
## Supplementary Figure 8



**Accumulation of *Caldaggef1<sup>+/-</sup>Rasa3<sup>hlb/hlb</sup>* platelets in spleen and liver. (A)** *Caldaggef1<sup>+/-</sup>Rasa3<sup>hlb/hlb</sup>* (black bars) or *Caldaggef1<sup>+/-</sup>Rasa3<sup>+/+</sup>* control platelets (open bars) were radiolabeled with Copper-64 and transfused into WT recipient mice (n=3). Twenty-four hours post transfusion, organs were harvested and radioactivity was measured with a gamma-counter. Consistent with the increased clearance of *Rasa3* mutant platelets, platelet-associated radioactivity in blood samples at t=24 hrs was markedly lower in mice transfused with *Caldaggef1<sup>+/-</sup>Rasa3<sup>hlb/hlb</sup>* compared to controls (*Caldaggef1<sup>+/-</sup>Rasa3<sup>hlb/hlb</sup>* over *Caldaggef1<sup>+/-</sup>Rasa3<sup>+/+</sup>* = 0.45). To account for the blood remaining in the excised tissue, results were normalized to Copper-64 signals in peripheral blood of the respective mice. **(B)** Peripheral platelet counts at the indicated time points after splenectomy in *Rasa3<sup>+/+</sup>* and *Rasa3<sup>hlb/hlb</sup>* mice. (n=5).



## Supplementary Figure 9



**Aggregation response** of wild type (*WT*), *Caldaggef1<sup>-/-</sup> Rasa3<sup>hib/hib</sup>* (*Cdg1<sup>-/-</sup> Rasa3<sup>hib/hib</sup>*) or *Caldaggef1<sup>-/-</sup>* (*Cdg1<sup>-/-</sup>*) platelets to increasing doses of Par4 agonist peptide (Par4p) in the presence of vehicle (black traces) or of the P2Y12 inhibitor 2-MeSAMP (light blue traces). Results are representative of three independent experiments. Note the very limited effect of the P2Y12 inhibitor 2-MeSAMP on the aggregation response of *Caldaggef1<sup>-/-</sup> Rasa3<sup>hib/hib</sup>* when compared to *WT* or *Caldaggef1<sup>-/-</sup>* platelets. A similar result was observed when platelets were activated in the presence of the PI3-kinase inhibitor, wortmannin (not shown).

## VIDEO CAPTIONS

**Supplementary Video 1.** Formation of a hemostatic plug in an injured venule of a *wild-type* mouse.

**Supplementary Video 2.** Formation of a hemostatic plug in an injured venule of a *Caldaggef1*<sup>-/-</sup> mouse.

**Supplementary Video 3.** Formation of a hemostatic plug in an injured venule of a *Caldaggef1*<sup>-/-</sup> *Rasa3*<sup>h1b/h1b</sup> mouse.

**Supplementary Video 4.** Formation of a hemostatic plug in an injured venule of a *wild-type* mouse treated with clopidogrel bisulfate.

**Supplementary Video 5.** Formation of a hemostatic plug in an injured venule of a *Caldaggef1*<sup>-/-</sup> mouse treated with clopidogrel bisulfate.

**Supplementary Video 6.** Formation of a hemostatic plug in an injured venule of a *Caldaggef1*<sup>-/-</sup> *Rasa3*<sup>h1b/h1b</sup> mouse treated with clopidogrel bisulfate.